# Astrocytes protect primary neurons from THC-induced damage

MARSHALL PLAN SCHOLARSHIP

FINAL REPORT

Brooke Boisvert, BSc.
October 2021 – July 2022

**Host Institution:** Medical University of Vienna, Vienna
**Supervisor:** Univ.-Prof. Dr. Tibor Harkany and Dr. Erik Keimpema
Department of Molecular Neuroscience, Center for Brain Research

# ABSTRACT

The legalization of medical and recreational cannabis and cannabis-derived products has increased the availability and consumption of cannabis products worldwide. These products vary in concentrations of $\Delta^9$-tetrahydrocannabinol (THC), the main psychoactive component in cannabis, with some preparations containing upward of 95% THC. Understanding how THC exposure will affect the postnatal brain is of increasing importance as THC, a highly lipophilic molecule, is transferred through breast milk and has shown to be associated with decreased mental development and memory function in infants. Previous research has shown that postnatal hippocampal THC exposure leads to long-lasting reorganization of neuronal circuits and alterations to neuronal cellular bioenergetics, but little is known regarding the role early postnatal hippocampal astrocytes play following THC exposure.

Here, we sought to understand how THC affects postnatal hippocampal astrocytes and elucidate the relationship between these glia and local neuron populations following THC exposure. First, we identified the minimal expression of cannabinoid type 1 receptors ($CB_1R$) in postnatal day 3 and postnatal day 8 hippocampal astrocytes via *in situ* hybridization, suggesting alternative mechanisms of action for THC in these astrocyte populations. We then worked from previous data that noted increased astrocytes in specific layers of the hippocampus post-THC exposure, postulating that these increases may be a result of astrocyte proliferation or differentiation. No identifiable changes in proliferation or differentiation were found after an EdU staining and quantification of astrocyte markers GFAP and s100β. However, *in vitro* neuron-astrocyte co-cultures revealed that astrocytes attenuate plant-derived and synthetic THC induced neuronal death. Despite the preservation of neuronal survival at micromolar THC concentrations, THC still disrupted cellular metabolism, as western blot analysis revealed a decrease in the expression of two mitochondrial proteins, UQCRC2 and MTCO1. Overall, this study shows that postnatal hippocampal astrocytes mitigate neuronal death following THC exposure *in vitro*, though further work is needed to understand the mechanism of action by which this occurs.

# ACKNOWLEDGEMENTS

I would first like to express my sincerest gratitude to Univ.-Prof. Dr. Tibor Harkany and Dr. Erik Keimpema for allowing me to research under their guidance for the nine-month duration of my grant. Without their willingness to take a chance on a recent graduate from Texas, I would not have had to opportunity to experience the exponential scientific growth my time at the Center for Brain Research endowed upon me. Here, I developed an enhanced scientific literacy and grew in confidence to perform research autonomously. My scientific career will be built on the foundation they helped me establish, and I cannot thank them enough.

I would also like to thank Fulbright Austria and the Austrian Marshall Plan Foundation for their belief in my project proposal and their financial support of my research grant. I would especially like to thank Darrah Lustig for helping me navigate the bureaucratic steps of moving to Austria. Her assistance was key to a smooth transition in-country.

My time in Vienna was more than a scientific endeavor. The experiences I had within the Austrian community and my Fulbright cohort are memories that will last a lifetime. These people challenged my beliefs and pushed me outside of my comfort zone, expanding my perceptions of the world and catalyzing my personal growth. Little moments of happiness like afternoon coffee and cake to picnics on Kahlenberg became hallmarks of life in Vienna and helped me appreciate the Viennese way of life. In nine-months, Vienna became my home away from home, and its culture and people will forever hold a large place in my heart.

And lastly, I would like to thank my family and friends for their continuous encouragement of my loftiest dreams. I would not have been able to move halfway around the world without their ceaseless love and support.

## TABLE OF CONTENTS

# 1. INTRODUCTION

## 1.1 $\Delta^9$- tetrahydrocannabinol: THC

Cannabis is a psychoactive plant that has been utilized for functional, medicinal, and recreational purposes for thousands of years (Adams, 1942), with some of the earliest documentation of cannabis use dating back nearly 12,000 years ago in Central Asia (Crocq, 2020). However, it was not until the late 19th century that cannabis began to make its way to the Western hemisphere where it has been used in the treatments of tetanus, rheumatism, and convulsions (O'Shaughnessy, 1843). Today, over 188 million adults worldwide, nearly 4% of the global adult population, report cannabis use. These numbers continue to rise as legalization in many regions has decreased the retail price of cannabis and increased its availability (Lynskey et al., 2012).

Cannabis contains over 100 cannabinoids (Crocq, 2020). In cannabis, these cannabinoids are referred to as phytocannabinoids, with each of these phytocannabinoids composed of a molecule containing a 21-carbon terpenophenolic carbon skeleton (Chayasirisobhon, 2020). Within the cannabis plant, the most abundant of these phytocannabinoids are cannabidiol (CBD) and $\Delta^9$- tetrahydrocannabinol (THC). While CBD is nonpsychotropic, THC is known for being the primary psychotropic component found within cannabis (Felder et al., 1998). Following the discovery of THC in 1964 by Mechoulam and Gaoni, elucidating the mechanism of action from THC became of increasing importance, leading to the discovery of the endocannabinoid system.

## 1.2 Endocannabinoid system

The characterization of the endocannabinoid system began with the discovery of the cannabinoid type 1 receptor ($CB_1R$) by Devane et al in 1992 and has since emerged as a key neuromodulatory system. Within the endocannabinoid system lies a series of components, with each of these components playing a critical role in modulating synaptic transmission. These include endogenous cannabinoids, cannabinoid receptors, and enzymes involved in synthesis and degradation of endogenous cannabinoids (Lu et al., 2016).

Today, there are two primary mediators of the endocannabinoid system: $CB_1R$ and $CB_2R$. Both the $CB_1R$ and $CB_2R$ are 7-transmembrane G protein coupled receptors that work primarily via the inhibitory $G_i$ and $G_o$ G proteins and are activated by endogenous cannabinoids and other agonists, including THC. While the $CB_2R$ is found primarily in immune cells and peripheral tissues, the $CB_1R$ has been found to be the primary cannabinoid receptor within the central nervous system (Howlett et al., 2002). It is within the central nervous system that the stimulation of the $CB_1R$ induces the psychoactive effects of THC. The bioactivities of THC at the $CB_1R$ are known to vary as stimulation has been shown to be neuroprotective through the pre-synaptic inhibition of glutamate release while other studies suggest that this reduction of glutamate, specifically in the hippocampus, may be involved in the disruption of learning and memory through the inhibition of synaptic plasticity. (Gomez et al., 2002) (Bliss & Collingridge et al., 1993). With one study showing that $CB_1R$ knock-out mice have disrupted axon development and

pathfinding in pre- and postnatal neurodevelopment, a high priority has been placed on understanding how THC and the $CB_1R$ interact in developing brain (Mulder et al., 2008).

## 1.3 THC exposure during neurodevelopment

THC acts as a partial agonist at the $CB_1R$ and $CB_2R$ (Pertwee et al., 2008), though the vast expression of $CB_1R$ in the brain renders it a primary mediator of action for THC (Huestis et al., 2007). In mammals, the $CB_1R$ is expressed early on in embryonic development, seen even before the development of the neural tube and neuroectoderm (Sun et al., 2008). Later in neural development, $CB_1R$ expression is seen in the telencephalon at embryonic day 11.5 (E11.5) and the cortex and hippocampus beginning at E13.5 – E14.5 (Morozov et al., 2009). This early $CB_1R$ expression has been shown to be a key modulator in axon pathfinding and neurogenesis throughout neurodevelopment (Crittenden et al., 2022).

Understanding the molecular determinants through which THC disturbs neurodevelopment is of increasing importance as THC, a highly lipophilic molecule, is transferred through breast milk. As cannabis and cannabis-products become increasingly available through legalization, the prevalence of marijuana usage is increasing, with 14% of adults in the United States using marijuana in 2014 compared to 10% in 2008 (Compton et al., 2016). Furthermore, the increase in consumption has been seen in parallel with increases in the percentage of THC in cannabis. In a study done by the National Institute of Health in 2020, cannabis samples seized from the Drug Enforcement Administration from 1995 to 2019 showed a decrease in the percentage of CBD contained in the cannabis and an increase in the THC percentage, rising from 3.96% THC in 1995 to 14.35% THC in 2019 (NIH, 2020). In addition, new preparations of cannabis oils, such as e-cigarettes, have provided safe smoking alternatives that have THC concentrations upwards of 95% (Zhang et al., 2016) Therefore, understanding how cannabis exposure will affect postnatal brain maturation is of pressing relevance.

Data from human longitudinal studies looking at postnatal exposure to THC have indicated decreased motor skills, reduced executive control, academic functioning, and impaired learning in adolescents. (Astley et al., 1990) (Scott et al., 2017) (Becker et al., 2017) (Castellanos-Ryan et al., 2017). Additionally, anatomical data collected from low dose THC usage adolescents has shown that in addition to the behavioral effects, THC exposure increases gray matter volume, which correlated with the future presentation of generalized anxiety symptoms (Orr et al., 2019). These studies and others showing negative implications of cannabis use during brain maturation has catalyzed the scientific push to elucidate the molecular mechanisms and cellular alterations induced by cannabis.

Some studies looking at cannabinoid receptor signaling suggest that THC acts by targeting the mitochondria, in turn affecting cellular metabolism (Melser, 2017) (Bénard, 2012). Within pulmonary cells, both THC and cannabis smoke were found to diminish mitochondria membrane potential (Sarafian et al., 2003). Similar data was discovered in striated muscle cells as THC reduced mitochondrial function and the genetic deletion of $CB_1Rs$ resulted in an upregulation of pyruvate metabolism-associated enzymes (Fišar et al., 2014). This data has sparked a debate about whether the effect of THC is mediated by $CB_1Rs$ or if THC itself can change mitochondrial membranes directly (Fišar et al., 2014). Current data suggests that THC

alters membrane integrity and alters ATP processing, with as little as a single dose of THC altering lipid metabolism in both adolescent and adult mice (Hillard et al., 1985) (Leishman et al., 2018). Despite these defined changes, there has yet to be a direct link established between the metabolic effects of THC-mediated signaling and morphological impairments. However, a large-scale proteomics dataset revealed a majority of targets (>58%) associated with cellular and mitochondrial metabolic proteins are affected by THC exposure in juvenile mice. This dataset also revealed an increase in excitatory amino acid transporter 2 (EAAT2) expression in response to THC exposure (Beiersdorf et al., 2020). As a major glutamate transporter expressed predominately in astroglia, this data suggests increases in astrocyte populations in response to THC exposure, but further research is needed to better uncover the relationship between THC and astrocytes in early postnatal development.

# 2. ASTROCYTES

## 2.1 Role of astrocytes in the CNS

In mammals, glial cells are found in roughly equal proportions to neurons and are comprised of astrocytes, radial glia, oligodendrocyte progenitor cells, oligodendrocytes, and microglia (von Bartheld et al., 2016). Within the central nervous system, astrocytes are defined by their characteristic starshaped morphology and their interaction with a variety of cell types. Functionally, astrocytes play a role in maintaining the homeostasis of the central nervous system by regulating the blood brain barrier, recycling neurotransmitters, and secreting trophic factors (Weber et al., 2015). Their function also extends to the regulation of blood flow and ion balance, which assists glucose travel between neurons (Sims et al., 2017) (Timper et al., 2020).

## 2.2 Astrocytes and THC

The presence of $CB_1R$ in astrocytes has been the subject of a great deal of controversy. While some studies have shown relatively low expressions of $CB_1R$ throughout the hippocampus (Gutierrez-Rodriguez et al., 2018), the caudate putamen (Rodriguez et al., 2001), the neocortex (Zhang et al., 2014) and the spinal cord (Hegyi et al., 2009), others argue that there is little functional expression of $CB_1R$ via *in situ* hybridization (Navarette et al., 2014).

In addition to the $CB_1R$ located on the plasma membrane, astrocytes have been shown to have $CB_1R$ located on intracellular organelles such as the mitochondria (Gutierrez-Rodriguez et al., 2018). Activation at these astroglial mitochondrial $CB_1R$ ($mtCB_1R$) regulate mitochondrial respiration through the inhibition of cAMP/PKA signaling and decreased phosphorylation of the mitochondrial complex I. This reduces the stability of complex I and alters the production of reactive oxygen species (ROS) (Vicente-Gutiérrez et al., 2021), which ultimately results in reduced glycolytic capacity and increases bioenergetic stress (Jimenez-Blasco et al., 2020).

Further investigation of $CB_1R$, THC, and astrocytes is needed to draw conclusions about their relationship in neurodevelopment. Given the high levels of neurons, reactive astrocytes and $CB_1R$ present in the hippocampus, early postnatal hippocampal neurons and astrocytes were

chosen as our experimental population (Fuerte-Hortigón et al., 2021) Furthermore, with the hippocampus playing a major role in learning in memory, astrocytes and neurons in the developing hippocampus were of keen interest, as THC stimulation of astrocyte $CB_1R$ has been shown to activate abnormal neuronal activities and result in poor memory (Chen et al., 2013). Preliminary data from our lab had also shown increased levels of s100β and GFAP positive astrocytes in the stratum radiatum of the postnatal hippocampus following THC exposure. This was found alongside iTRAQ proteomics data indicating increased levels of excitatory amino acid transporter 2 (EAAT2), a glutamate transporter expressed predominately in astrocytes, following postnatal THC exposure *in vivo.* These changes were seen in conjunction with data from Beiersdorf et al that demonstrated early postnatal THC exposure resulted in thinning of the hippocampal CA1 pyramidal layer and a decrease in interneurons in the stratum oriens and the stratum lacunosum moleculare. Together, the increased levels of astrocyte markers in surrounding hippocampal regions coupled with decreased neuron populations led to our hypothesis that astrocytes may respond to THC in the early postnatal hippocampus by proliferating, differentiating, or migrating in response to THC-induced environmental stress.

Here, we work to show how THC affects early postnatal hippocampal astrocyte populations using an *in vitro* system. Using this method, we are better able to control and study the responses of these specific hippocampal cell populations, highlighting how THC affects proliferation and differentiation in astrocytes and how the presence of astrocytes *in vitro* with neurons alters neuronal survival and neurite outgrowth. Lastly, we will show how oxidative phosphorylation (OXPHOS) machinery is affected by THC *in vitro* among neurons and neuron-astrocyte cultures.

# 3. AIMS

The overall goal for my project is to elucidate the relationship between early postnatal hippocampal astrocytes and neurons following exposure to THC. To do this, we will use an *in vitro* model to study astrocyte proliferation and differentiation before analyzing how the presence of astrocytes in a neuronal culture affects survival and cellular metabolism proteins.

Previous work in the lab found that postnatal hippocampal plant-derived THC (pTHC) exposure alters the assembly of cortical networks in offspring prenatally exposed to pTHC. Furthermore, this exposure resulted in the thinning of the CA1 hippocampal region of the juvenile hippocampus (Beiersdorf et al., 2020). This data suggests that pTHC is averse to hippocampal development in neuronal populations, but little is known about how THC exposure affects postnatal hippocampal astrocytes. At the beginning of my study, we must first verify the presence of the $CB_1R$ in the astrocyte populations. This will be done using *in situ* hybridization on early postnatal hippocampal tissue from C57Bl6/J mice using $CB_1R$ and GFAP probes. The presence or absence of colocalization for these probes will allow for the determination of the presence of $CB_1R$ on astrocytes. Next, we will culture early postnatal astrocytes and subject these populations to pTHC for one-day and three-days. Immunohistochemical staining and imaging of these astrocytes following the one-day and three-day incubation period with pTHC will provide quantifiable data regarding proliferation and differentiation.

Next, we will investigate the relationship between early postnatal hippocampal astrocytes and neurons following exposure to various concentrations of pTHC and synthetic THC (sTHC). In postnatal hippocampal neurons alone, pTHC and sTHC disrupted the neuronal plasma membrane of the neurons, resulting in increased neuronal death the higher the concentration of THC (Beiersdorf et al., 2020). My project will look to understand how acute exposure to pTHC and sTHC alters astrocyte survival *in vitro*. Using an IncuCyte live-cell imaging device, we will create an experiment that exposes postnatal hippocampal astrocytes, astrocytes and neurons, and neurons alone to varying concentrations of pTHC. Data will be collected over a period of three days and imaged in the IncuCyte every two hours. This experiment will help establish a critical concentration of pTHC where changes in the morphology and viability are identifiable within the cell culture. The subsequent experiment will repeat the experimental setup of the pTHC exposure but isolate the effects of THC by using sTHC, removing any variability associated with phytocannabinoids, terpenes, and flavonoids found within pTHC. Furthermore, variable amounts of astrocytes will be plated to identify a sensitive level of astrocytes needed for a biological effect.

In accordance with the hypothesis that THC induces cellular dysfunction, my next question centers around the metabolic impact of THC exposure on astrocytes. With the remaining time I have on my grant, I will quantify any changes in metabolic markers when THC is given to postnatal hippocampal neurons alone compared to a neuron-astrocyte co-culture. Western blot analyses will then be used to quantify the changes in oxidative phosphorylation proteins, which influence ATP production.

In summary, this project strives to elucidate the relationship between THC, astrocytes, and the neuron-astrocyte relationship in the postnatal hippocampus.

# 4. METHODS

*Drugs*
Plant-derived, highly-purified THC (pTHC; 314.46 mg/mol, 95% purity) was provided in ethanol by GW Pharmaceuticals. Synthetic THC (sTHC) was obtained from THC Pharm (diluted in methanol with 98.9% purity or ethanol with 99.4% purity) and from Lipomed (in ethanol with > 97% purity). For drug preparations, sTHC was diluted from 75 mM stock into and aliquoted into 10mM concentrations in dimethyl sulfoxide (DMSO; Sigma) and stored at -80°C.

*Fixed tissue preparation*
C57Bl6/J mice were perfusion fixed with 4% PFA at a flow rate of 5 mL/min for a total of 15 minutes using a Peri-Star Pro peristaltic pump (World Precision Instruments, PERIPRO-4L). This was preceded by a 3-minute infusion of NHDG-HEPES. Following fixation, brains were dissected out, postfixed in 4% PFA overnight at 4°C, and transferred into a 30% sucrose solution for at least 48 hours. The tissue was then sectioned coronally at a 50 μm thickness using a CryoStar NX70 Cryostat (Thermo Scientific) and placed into 12-well plate containing 2 mL of 1X PBS, 0.05% sodium azide solution and kept at 4°C.

*Fresh-frozen tissue preparation*
Brains from C57Bl6/J mice were dissected out and placed into cryomolds (Tissue-Tek) and covered with O.C.T. Compound (Tissue-Tek) before being stored at -80°C.

*Immunohistochemistry*
For immunohistochemistry, cells were collected from the incubator and placed on ice. Cells were then fixed in 4% PFA after removing the growth medium and washed once with PBS. Subsequent PBS washes to remove any remaining PFA were followed by 1 hour on blocking solution (NDS; Jackson ImmunoResearch, 1% BSA; Sigma, 0.2% Triton X-100; Sigma) to quench non-specific immunoreactivity. The cells were then exposed to primary antibodies diluted in PBS supplemented with 0.1% BSA (Sigma), 2% NDS (Jackson ImmunoResearch), and 0.2% Triton X-100 (Sigma) at 4°C for 24h. Multiple washes with PBS were performed before secondary IgGs tagged with DyLight Fluor 488, 560, or 633 fluorochromes (1:500; Jackson ImmunoResearch, RT for 2h) were introduced to the cells. A Hoechst 33,342 (Sigma) nuclear stain was used from nuclear identification. After multiple PBS washes, the coverslips were mounted on fluorescence-free glass slides glycerol gelatin (Sigma). Visualization of the fluorochromes were acquired on a LSM 880 confocal laser scanning microscope (ZEISS).

*Click-iT EdU*
Astrocytes were plated into a 24-well plate (25,000 cells/well; 0030730119, Eppendorf) with coverslips that were pre-treated with poly-D-lysine in 0.1M borate buffer overnight and allowed to recover overnight before additional treatment. Half of the medium in the wells was removed and replaced with a 2x EdU and THC or DMSO containing medium and left to sit incubate for one day and three days. After the allotted time, astrocytes were fixed in 4% PFA and washed with 3% BSA. Astrocytes were then permeabilized with 0.5% Triton X-100 in PBS. EdU was then visualized through the addition of the Click-iT reaction cocktail and imaging using a LSM 880 confocal laser scanning microscope (ZEISS).

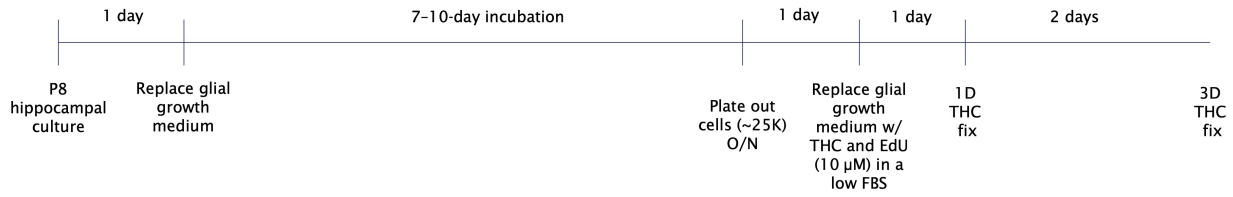


*In situ hybridization*

Fresh-frozen tissue was sectioned at a 16 μm thickness coronally using a CryoStar NX70 Cryostat (Thermo Scientific), collected on Superfrost Plus (Thermo Scientific) microscope slides, and stored at -20°C. For *in situ* hybridization, probe hybridization buffer (Molecular Instruments) was added on top of slides and pre-hybridized inside a humidified chamber at 37°C. A probe solution containing 0.4 pmol of each probe was added to probe hybridization buffer. The slides incubated in a humidified chamber at 37°C overnight after the probe/probe hybridization buffer solution was added to slides. The following day, coverslips were removed from the slides and excess probe was removed using a series of 4X probe wash buffer and 5 x SSCT washes at 37°C. The series of washes was followed by one, 5-minute 5 x SSCT wash at room temperature. For probe amplification, amplification buffer (Molecular Instruments) was added on top of each slide and then placed into a humidified chamber to pre-amplify for 30 minutes at room temperature. A hairpin solution was created during the pre-amplification step. This hairpin solution contained 6 pmol of hairpin h1 and 6 pmol of hairpin h2 and was made using 2 μL of 3 μM stock. The h1 and h2 hairpins were then heated to 95°C and cooled to room temperature in a dark drawer for 30 minutes. Once the slides had finished pre-amplifying and the hairpins were cooled, the snap-cooled h1 and h2 hairpins were added to 100 μL of amplification buffer at room temperature. The pre-amplification buffer was removed from the slides before 100 μL of hairpin mixture was added to the slide. A coverslip was placed on top of the slides and the samples were incubated in a dark humidified chamber room overnight at room temperature. The next day, the coverslips were removed, and excess hairpin was washed away with three 5 x SSCT washes: 2 X 30 min followed by 1 X 5 min. After the washes, antifade mounting reagent and coverslips were added on top of the slides. The slides were left to dry before imaged using a LSM 880 confocal laser scanning microscope (ZEISS).

*Astrocyte and neuronal co-cultures and IncuCyte imaging*

Astrocytes were isolated from P8 C57Bl6/J mouse hippocampi and grown in DMEM + GlutaMAX medium (GIBCO, Life Technologies) supplemented with penicillin-streptomycin (1%), sodium pyruvate (1%), fetal bovine serum (10%), and N2 supplement (1%). Medium was replaced after 24 hours to remove excess cellular debris. The astrocytes were then grownup to confluence (>1 week) in a T-75 flask (Thermo Scientific) before being plated out for experimental use. For co-cultures, the astrocytes were removed from the flask and isolated into a single-cell suspension with Neurobasal A medium (GIBCO, Life Technologies) supplemented with penicillin-streptomycin (1%), GlutaMAX (1%), and B27 supplement (2%), subsequently referred to as NBA+. The desired number of astrocytes were then plated out in 100 μL of NBA+ in 96-well plates or 1 mL in 12-well plates pre-treated with poly-D-lysine in 0.1M borate buffer overnight. Neurons were then collected from E14-E18 mouse hippocampi and cortex and were grown in NBA+. The neurons were plated out in the same 96-well plate or 12-well plate in 100 μL of NBA+ or 1 ml of NBA+ respectively. The co-culture incubated at 37°C overnight before introducing the THC or DMSO control. The THC and DMSO control were added by removing

half of the NBA+ medium from the wells and replacing with the same volume of THC/control containing medium. An IncuCyte live-cell imaging device (Essen Bioscience) was then used for live cell imaging over three days. Phase contrast images were taken every two hours. 'Cell-Body Cluster Area' was taken as a measure of cell viability and refers to the surface area occupied by cell bodies ($mm^2/mm^2$). Neurite growth was tracked using the 'Neurite Length' measure ($mm/mm^2$). The measures used for this experiment were optimized in preliminary experiments.

*Western blotting*

The THC treated astrocyte-neuronal co-culture was lysed and homogenized in cell lysis buffer (100 mM Tris, pH 7.4, 150 mM NaCl, 1 mM EGTA, 1 mM EDTA, 1% Triton X-100, 0.5% Sodium deoxycholate, 1x protease inhibitor, 1x phosphatase inhibitor) before preparing the total protein fractions. Protein concentrations were determined using the Pierce BCA Protein Assay Kit (Thermo Scientific). For protein analysis, 5.36 $\mu$g of each sample was used. Protein samples underwent a denaturation step at 95°C for 5 minutes. Samples were then loaded and run in a gel containing a 4% SDS stacking gel on top of a 10% SDS separation gel before being transferred onto a PVDF membrane. The membrane was blocked (5% skim milk powder (Sigma) in TBS-T) before primary antibodies were added to the membrane and left to incubate at 4°C overnight. Primary antibodies were removed through a series of TBS-T and TBS washes. Secondary antibodies were then added and incubated on then membrane for 1 hour at RT. Clarity Wester ECL Substrate (BioRad) was used for developing the HRP conjugated immunoblot and was visualized using the ChemiDoc MP Imaging System (BioRad).

For the western blot analysis, the PVDF membrane was stripped twice and reused with new primary and secondary antibodies. This was done by first washing off the Clarity Wester ECL Substrate used to develop the HRP conjugated immunoblot with a 5-minute TBS wash. Afterward, the PVDF membrane was immersed in Restore ™ Western Blot Stripping Buffer (Thermo Scientific) for 30 minutes before being washed again in TBS twice: one quick wash and one 5-minute incubation. The membrane was then re-blocked in 5% skim milk powder (Sigma) in TBS-T for one hour before proceeding with the western blot protocol with the addition of the primary antibody. Antibody concentrations for the western blots were as follows:

| | |
|---|---|
| 1° OXPHOS 1:500 (Rodent WB; Abcam) | 2° Mouse HRP 1:1000 (Jackson Immunoresearch) |
| 1° BIII Tubulin 1:3000 (Promega) | 2° Mouse HRP 1:2000 (Jackson Immunoresearch) |
| 1° GFAP 1:1000 (Synaptic Systems) | 2° Guinea Pig HRP 1:1000 (Jackson Immunoresearch) |

*Statistical Analysis*

Statistical significance between the groups was analyzed with unpaired two-tailed t-test. *P=<0.05. **P=<0.01.

# 5. RESULTS

## 5.1 Minimal $CB_1R$ in hippocampal astrocytes

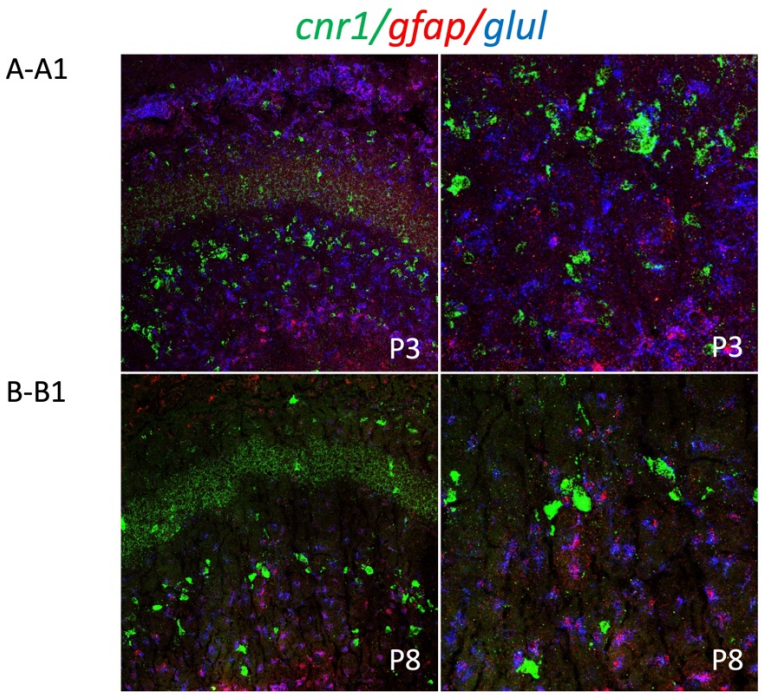


**Figure 1**: *In situ* hydridization of postnatal day 3 (A-A1) and postnatal day 8 (B-B1) mouse hippocampus indicated minimal colocalization of the cannabinoid receptor type 1 (*cnr1*) with astrocytic markers glial fibrillary acid protein (*gfap*) and glutamine synthase (*glul*).

To establish the relationship between the $CB_1R$ and postnatal hippocampal astrocytes, *in situ* hybridization was performed on postnatal hippocampal tissue from C57Bl6/J mice at two early developmental time points: postnatal day 3 and postnatal day 8. In neurons, the $CB_1R$ is identifiable as early as embryonic day 12.5 (Vitalis et al., 2008) whereas the expression of functional cannabinoid receptors in astrocytes remains poorly understood. Some evidence suggests that $CB_1Rs$ are present in the caudate putamen (Rodriguez et al., 2001) and the dorsal horn of the spinal cord (Salio et al., 2002), while some suggest that there are no $CB_1R$ in astrocytes (Stella, 2004). To determine the presence or absence of the $CB_1R$ in the postnatal hippocampus, three *in situ* hybridization probes were used: *cnr1, gfap,* and *glul. Cnr1* is the protein coding gene for the $CB_1R$, *gfap* is the protein coding gene for the glial fibrillary acidic protein, which is an intermediate filament protein that provides support and strength to astrocytes and is seen in activated astrocytes, and *glul* is the protein coding gene for glutamine synthetase that catalyzes the ATP-dependent conversion of glutamate and ammonia to glutamine and is predominately expressed in astrocytes (Anlauf et al., 2013). These markers effectively localize the expression of the $CB_1R$ gene and genes commonly found in astrocytes within the hippocampus.

*In situ* hybridization for the postnatal day 3 and 8 hippocampal tissue revealed that there is minor presence of the *cnr1* gene in a subset of *gfap/glul* expressing astrocytes, with the majority of astrocytes containing undetectable *cnr1* levels in this experimental setting. This data suggests that at this developmental stage, some astrocytes could indeed respond to THC, but alternative mechanisms would most likely affect the remaining bulk.

The limited amount of $CB_1R$ within astrocyte populations does not inhibit the ability of THC to work within these cell populations. Despite the $CB_1R$ being the predominate cannabinoid receptor in the hippocampus, additional mechanisms of action include binding to the cannabinoid type 2 receptor ($CB_2R$), other G-protein coupled receptors, transient receptor potential channels, peroxisome proliferator-activated receptors, and monoamine transporters (Lutz, 2004). Furthermore, the identification of $mtCB_1R$ yields an additional subcellular receptor that the lipophilic THC may work through in these developing astrocytes (Harkany et al., 2017).

## 5.2 Stimulation of astrocytes with pTHC *in vitro*

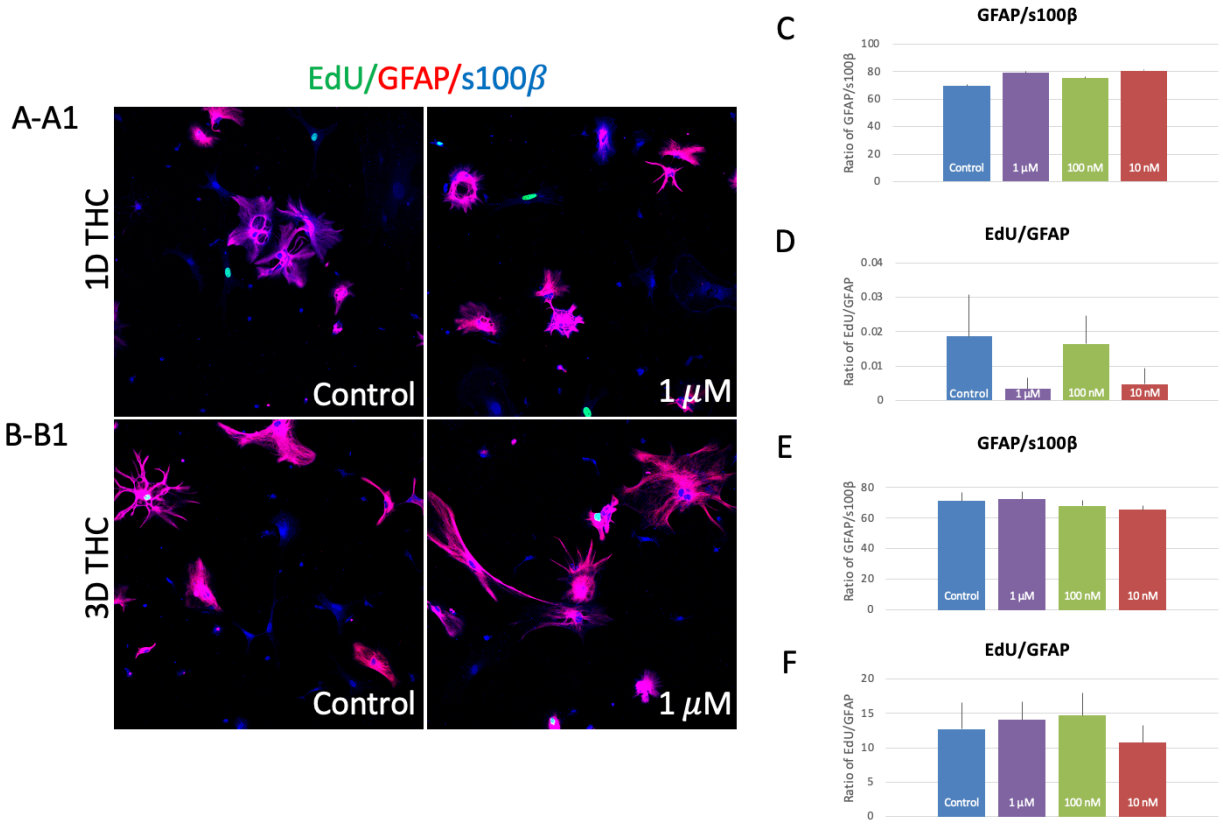


**Figure 2**: Immunohistochemistry of astrocytes exposed to DMSO (control) or pTHC (1 $\mu$M) for 1 day (A-A1) and 3 days (B-B1). (C) 1 $\mu$M pTHC resulted in no significant increase in GFAP and s100$\beta$ labelled astrocytes, and no change in the ratio of GFAP/s100$\beta$ for the 1-day pTHC condition. (D) There were no changes in the ratio of EdU/GFAP between the control, 1 $\mu$M, 100 nM, and 10 nM for the 1-day pTHC condition. (E) 1 $\mu$M pTHC resulted in no significant increase in GFAP and s100$\beta$ labelled astrocytes, and no change in the ratio of GFAP/s100$\beta$ for the

3-day pTHC condition. (F) There were no changes in the ratio of EdU/GFAP between the control, 1 $\mu$M, 100 nM, and 10 nM for the 3-day pTHC condition.

An *in vitro* postnatal hippocampal astrocyte model was established to isolate and identify the cellular changes induced by THC exposure. iTRAQ proteomics data acquired from Beiersdorf et. al. revealed that increased levels of EAAT2 were found in the postnatal hippocampus in response to THC exposure. Responsible for the uptake of glutamate, EAAT2, or excitatory amino acid transporter 2, is found predominantly in astroglia. This data is further subsidized by findings in our lab that showed an increased amount of GFAP positive and s100$\beta$ positive cells in the stratum radiatum of the hippocampus post-THC exposure. The increases in these markers allude to changes in astroglia following pTHC exposure. We hypothesized that the increase in these astroglia markers may be attributed to proliferation, differentiation, or migration. We sought to identify these changes *in vitro*, using immunohistochemical techniques to visualize and quantify proliferation and differentiation specifically.

Astrocytes cultured from postnatal day 8 hippocampal tissue from C57Bl6/J mice were isolated and grown up in glial growth medium for 7-10 days. During this time period, the astroglia grew to confluence, at which point they were plated out into two pre-treated poly-D Lysine 12-well plates. Each well contained approximately 25,000 astrocytes. These cells incubated overnight in the original glial medium. The following day, the glial medium was replaced with DMEM containing pTHC (1 $\mu$M, 100 nM, or 10 nM) or the control (DMSO). Both of the plates were simultaneously treated with EdU. The first of the two plates was collected one-day post-THC treatment, fixed in 4% PFA, and left in PBS in the fridge. The second plate was then collected two days later, three-days post-THC treatment, where it was then fixed with 4% PFA and left in PBS. Both plates subsequently underwent the protocol for immunohistochemistry.

Three immunohistochemical markers were chosen for this analysis. Proliferation was measured using an EdU click-iT reaction. This reaction is a highly effective proliferation detection method that utilizes the incorporation of 5-ethynyl-2'-deoxyuridine into replicating DNA. This nucleoside analog is then fluorescently labeled with a fluorophore via click-iT reaction. This technique is sensitive and specific for proliferating DNA (Allen et al., 2013). The second marker we chose was GFAP. GFAP, or glial fibrillary acidic protein, is an intermediate filament-III protein present within astrocytes in the central nervous system. Its function as an intermediate filament protein allows for the visualization of astrocyte morphology (Hol et al., 2015). Additionally, GFAP plays a significant role in astrocyte activation (astrogliosis). Astrogliosis occurs in response to neural injury as astrocytes increase in size and protein expression to attend to the damaged areas (Yang et al., 2020). GFAP-containing astrocytes are also shown to contain neural stem cell potential. This is in contrast to s100$\beta$, our third immunohistochemical marker, which is characterized as a late developmental astrocyte marker characteristic of a mature astrocyte (Raponi et al., 2007).

Astrocytes exposed to one-day pTHC *in vitro* showed no changes in the ratio of GFAP/ s100$\beta$ astrocytes between the control, 1 $\mu$M, 100 nM, or 10 nM conditions. Furthermore, there were no significant differences in the EdU/GFAP ratio between the control, 1 $\mu$M, 100 nM, or 10 nM conditions. The three-day pTHC exposure mirrored the results found in the one-day

condition as there were no significant differences in the in the ratio of GFAP/ s100$\beta$ astrocytes between the control, 1 $\mu$M, 100 nM, or 10 nM conditions and no significant differences in the EdU/GFAP ratio between the control, 1 $\mu$M, 100 nM, or 10 nM conditions. This data works against our hypothesis that pTHC exposure in postnatal hippocampal astrocytes leads to changes in proliferation or differentiation.

## 5.3 IncuCyte imaging of neuron and neuron-astrocyte cultures

### 5.3.1 pTHC

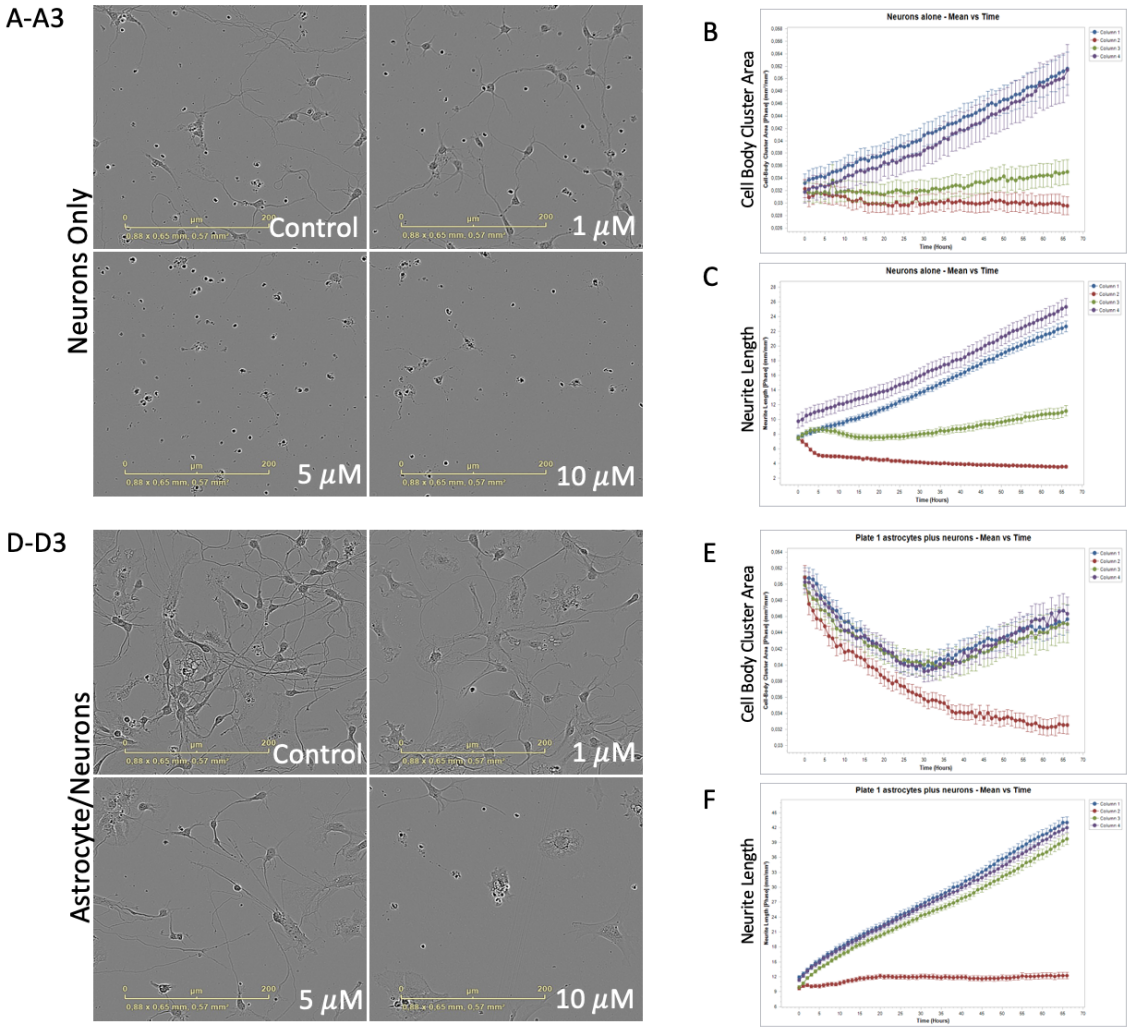


**Figure 3:** (A-A3) Incucyte imaging of neurons exposed to (A) DMSO (control), (A1) 1 $\mu$M pTHC, (A2) 5 $\mu$M pTHC, and (A3) 10 $\mu$M pTHC. (B) 5 $\mu$M pTHC and 10 $\mu$M pTHC resulted in a significant decrease in cell body cluster area ($mm^2/mm^2$) compared to the 1 $\mu$M pTHC and DMSO control. (C) Neurite length ($mm/mm^2$) decreases in 5 $\mu$M pTHC and 10 $\mu$M pTHC. (D-D3) Incucyte imaging of co-cultured astrocytes and neurons exposed to (D) DMSO (control), (D1) 1 $\mu$M pTHC, (D2) 5 $\mu$M pTHC, and (D3) 10 $\mu$M pTHC. (E) The presence of astrocytes

maintains cell body cluster area in 5 $\mu$M pTHC and delays the decrease in cell body area in 10 $\mu$M pTHC. (F) 5 $\mu$M pTHC retains neurite length. 10 $\mu$M pTHC yields minimal neurite growth.

Discrete time-intervals were chosen for data collection for astrocyte immunohistochemistry. Given as we were unable to identify changes in proliferation or differentiation at these time-points, we utilized the IncuCyte live-cell imaging incubator to provide morphological data of the neurons and astrocytes throughout the entire 72-hour duration of the experiment.

Two cultures were created for this experiment. The first was a neuron only culture containing 150,000 neurons per well that was subjected to either a DMSO control, 1 $\mu$M pTHC, 5 $\mu$M pTHC, or 10 $\mu$M pTHC condition. In each paradigm, cell body cluster area and neurite length were recorded every two hours throughout the 72-hour duration of the experiment. These measurements are noted as being key parameters in establishing THC toxicity (Keimpema et al., 2011). Graphical analysis of the neuron-only culture revealed that in the 1 $\mu$M pTHC condition, the cell body cluster area increased at the same rate as the control condition while the 5 $\mu$M and 10 $\mu$M pTHC experienced minimal cell body cluster area growth following the pTHC exposure, with the 5 $\mu$M only having a slightly greater increase in cell body cluster area growth compared to the 10 $\mu$M. Analysis of the neurite length showed that neurite growth is minimal in 5 $\mu$M pTHC and 10 $\mu$M pTHC compared to the control and 1 $\mu$M pTHC conditions.

These conditions were replicated for the neuron-astrocyte co-culture that contained 100,000 neurons and 50,000 astrocytes per well. Unlike the neuron-only culture that saw a reduction in cell body cluster area for the 5 $\mu$M pTHC and 10 $\mu$M pTHC, the neuron-astrocyte culture attenuated the effects of the 5 $\mu$M pTHC, as the cell body cluster area did not decline as seen in the neuron-only culture but mirrored the growth seen within the control and 1 $\mu$M pTHC conditions. Furthermore, analysis of the neurite length showed that the presence of astrocytes again reduced the impact of the 5 $\mu$M pTHC as it had a similar neurite length compared to the control and 1 $\mu$M pTHC conditions.

## 5.3.2 sTHC

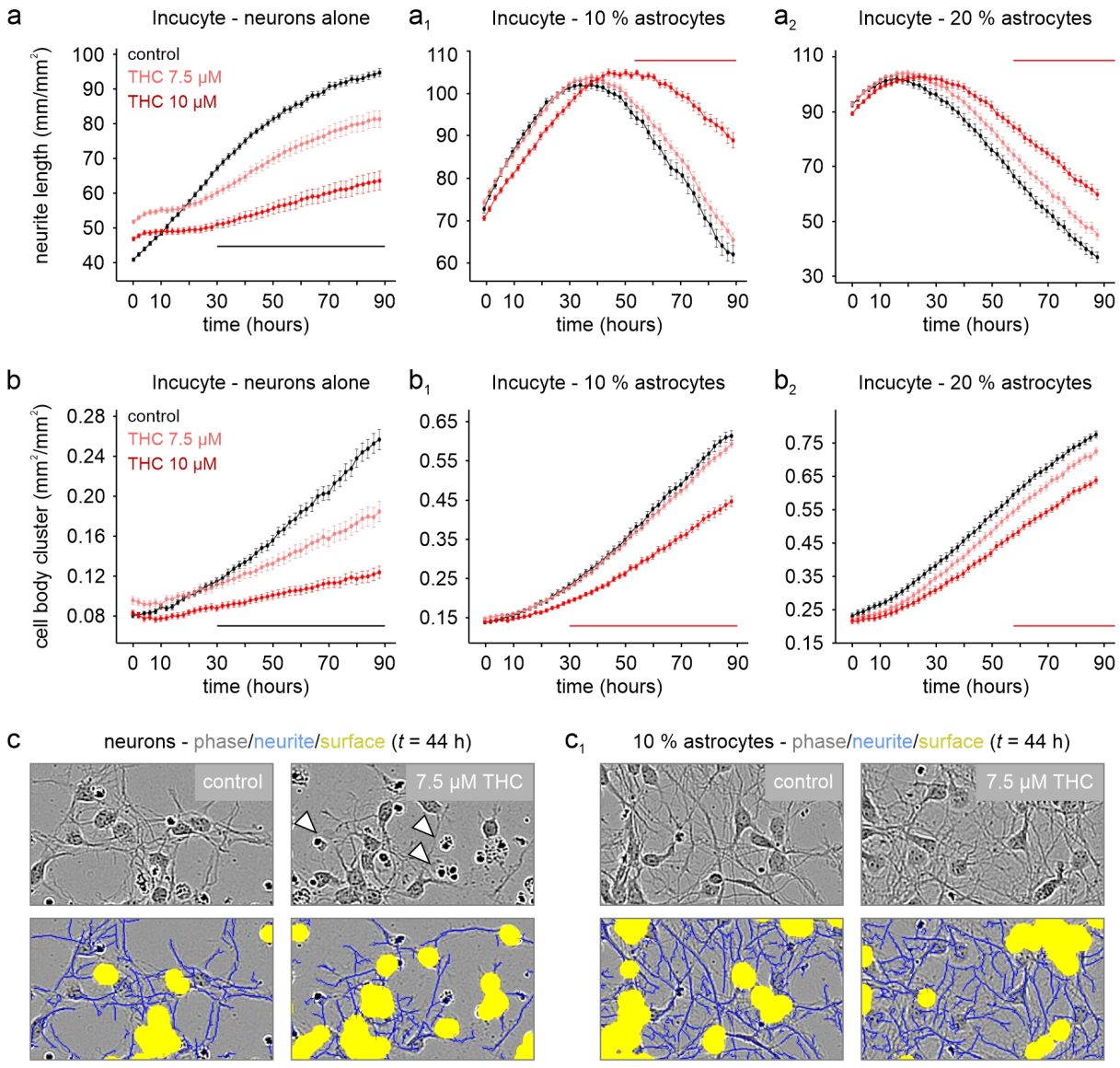


**Figure 4:** (A-A2) Analysis of neurite length (mm/mm$^2$) for neuron only, neuron + 10% astrocyte, and neuron + 20% astrocyte cultures exposed to DMSO, 7.5 $\mu$M sTHC, and 10 $\mu$M sTHC. (A) Neurite length decreases with increased sTHC concentrations. (A1) 10% astrocytes rescue neurite length in the 7.5 $\mu$M sTHC condition. (A2) 20% astrocytes rescue neurite length in the 7.5 $\mu$M and 10 $\mu$M sTHC condition. (B-B2) Analysis of cell body cluster area (mm$^2$/mm$^2$) for neuron only, neuron + 10% astrocyte, and neuron + 20% astrocyte cultures exposed to DMSO, 7.5 $\mu$M sTHC, and 10 $\mu$M sTHC. (B) Cell body cluster area decreases with increased sTHC concentrations. (B1) 10% astrocytes rescue cell body area in the 7.5 $\mu$M sTHC condition. (B2) 20% astrocytes increase cell body area in the 7.5 $\mu$M and 10 $\mu$M sTHC condition compared to the neurons alone. (C) IncuCyte image of neuron only culture detailing neurites and cell body

surface area for the control and 7.5 $\mu$M sTHC condition. (C1) IncuCyte image of neuron + 10% astrocyte culture detailing neurites and cell body surface area for the control and 7.5 $\mu$M sTHC condition.

While IncuCyte data analyzed in Figure 3 highlights the role astrocytes play in neural growth and survival following pTHC exposure, the presence of various phytocannabinoids, terpenes and flavonoids present within pTHC limits our ability to confidently discern whether the alterations to neural populations can be attributed to THC or other biologically active contaminants. We removed these confounds by creating new *in vitro* paradigms using sTHC with >99% THC purity.

Additionally, the *in vitro* cultures contained variable percentages of astrocytes. Three conditions were established: 0%, 10%, and 20% astrocytes. This model enables the identification of sensitive ratios of astrocytes and neurons at which neural survival and growth is preserved in the presence of variable concentrations of THC. The concentrations of sTHC were also changed to 7.5 $\mu$M and 10 $\mu$M sTHC as opposed to the 1 $\mu$M pTHC, 5 $\mu$M pTHC, or 10 $\mu$M pTHC used in the first experiment. These two values were chosen as critical concentrations where we hypothesized that sTHC may induce a marked decrease in neurite growth and cell body cluster area. This hypothesis is supported by the pTHC data shown in Figure 3 as well as previous work in the lab by Beiersdorf et al that revealed catastrophic membrane failure of statistical significance beginning at 7.5 $\mu$M pTHC.

Two neuronal measurements were analyzed following a 90-hour incubation period: neurite length and cell body cluster area. The identification of cell bodies and neurites was standardized at 44 hours and is shown in Figure 4 C-C1. Analysis of neurite length in the neuron only culture showed decreased neurite length over time in the 7.5 $\mu$M sTHC and 10 $\mu$M sTHC compared to the control. Furthermore, the 10 $\mu$M sTHC had less neurite growth compared to the 7.5 $\mu$M sTHC condition. However, in the presence of 10% and 20% astrocytes, the rate of neurite growth is conserved following exposure to 7.5 $\mu$M sTHC (Figure 4A1-A2) and 10 $\mu$M sTHC (Figure 4A2). A similar conservation of cell body cluster area can be seen in the 10% and 20% astrocyte conditions in the presence of 7.5 $\mu$M and 10 $\mu$M sTHC

Data from the sTHC experimental paradigm supports the findings seen in the pTHC experiment. However, it appears that high concentrations of sTHC (10 $\mu$M) are less detrimental compared to the same concentration of pTHC, with greater rates of growth seen in the measurements of neurite length and cell body cluster area in the sTHC neuron only and neuron + astrocyte conditions compared to the pTHC neuron only and neuron + astrocyte conditions. This may be attributed, in part, to the synergistic effects of phytocannabinoids and terpenes that may be present within the pTHC (Russo et al., 2011).

## 5.4 THC and cellular bioenergetics

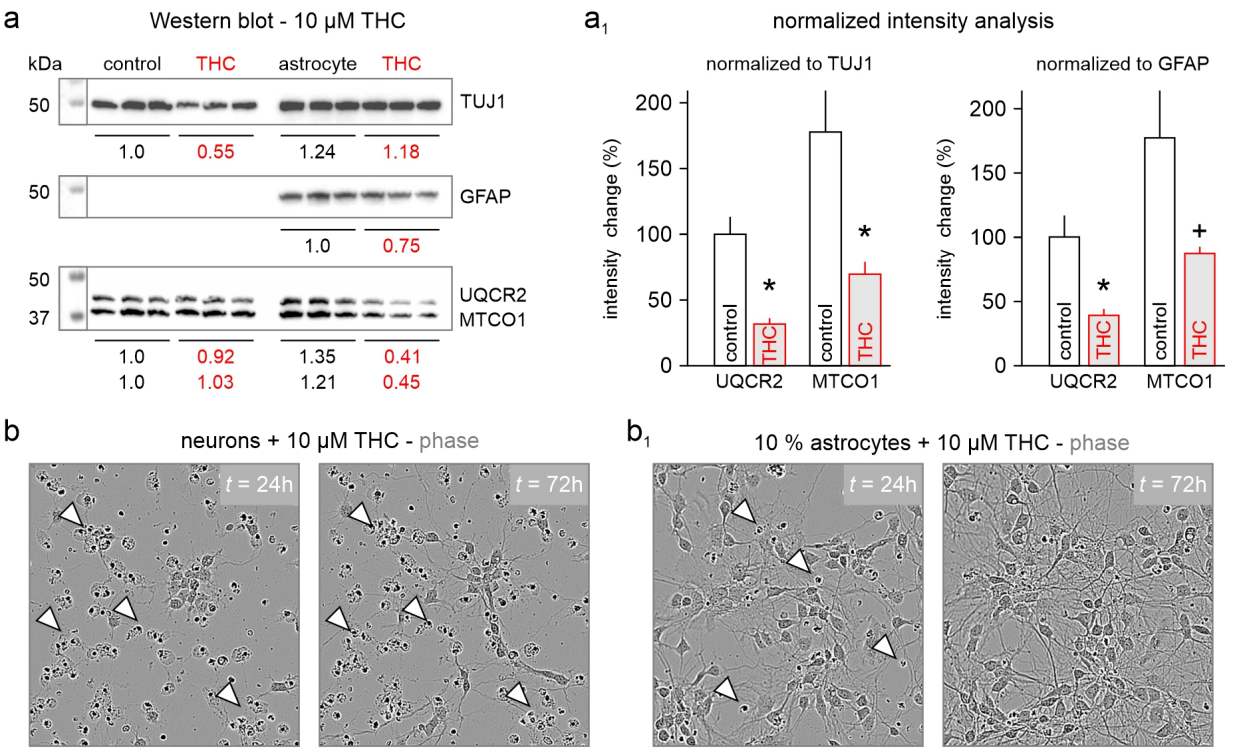


**Figure 5:** (A) Western blots from neuron and neuron + 10% astrocyte cultures exposed to DMSO control and 10 $\mu$M sTHC. TUJ1, UQCRC2, and MTCO1 intensities are normalized to the neuron only DMSO control for the respective blots and GFAP intensities are normalized to the neurons + 10% astrocyte DMSO control in the GFAP blot. TUJ1 decreases in intensity in the sTHC condition compared to the control for the neuron only culture. A similar decrease is not seen when comparing the control and the sTHC condition in the neurons + 10% astrocyte condition. Images of the GFAP marker show no presence in the neuron only culture and a 25% decrease in GFAP intensity in the sTHC condition compared to the control. There is no significant difference in the neuron only culture control and sTHC condition for UQCRC2 and MTCO1. However, there is significant intensity decrease in the neurons + 10% astrocyte sTHC condition for UQCRC2 and MTCO1 compared to the control. (A1) Analysis of UQCRC2 normalized to TUJ1 and GFAP show a significant decrease in intensity for UQCRC2 when exposed to sTHC in the neurons + 10% astrocyte culture. A significant decrease in MTCO1 is seen when normalized to TUJ1 and a trending decrease is seen when normalized to GFAP. (B) IncuCyte images of neuron only cultures exposed to 10 $\mu$M sTHC for 24 and 72 hours. (B1) IncuCyte images of neurons + 10% astrocyte cultures exposed to 10 $\mu$M sTHC for 24 and 72 hours.

One hypothesis for neural death following THC exposure is the disruption of cellular metabolism. In an iTRAQ proteomics analysis of the preadolescent brain following pTHC

exposure, 5 proteins involved in cellular respiration were found to be upregulated. The increase in these proteins was thought to be reactionary to overcome mitochondrial stress as a result of pTHC action. Exposure to 1 and 5 mg/kg THC at postnatal day 48 yielded an upregulation in mitochondrial complexes I, III, and V and subunits, validating the finding of the iTRAQ proteomics analysis (Beiersdorf et al., 2020).

The data from Beiersdorf et al was collected using a total protein extraction from preadolescent hippocampus. To better isolate how this machinery is affected in specific cell populations, we collected protein for western blot analysis from cultured neurons and neurons + 10% astrocytes.

First, we used western blot to quantify known neuron (TUJ1) and astrocyte (GFAP) markers within a neuron only and neuron + 10% astrocyte culture. TUJ1 identities β-III Tubulin and is a marker widely used to differentiate neurons from other cell types (Lee et al., 2005) while GFAP is an intermediate filament protein used to identify astrocytes (Zhang et al., 2017). In alignment with the IncuCyte data shown in Figure 3 and Figure 4, we saw a significant decrease in the expression of TUJ1 in the neuron only condition exposed to 10 $\mu$M sTHC and no change in expression in the neuron + 10% astrocyte condition exposed to 10 $\mu$M sTHC. The preservation of TUJ1 expression in the neuron + 10% astrocyte also supports the preservation of cell body area and neurite outgrowth seen previously. In addition, the GFAP staining verifies the presence and absence of astrocytes within the neuron + 10% astrocyte condition and neuron control respectively. A 25% decrease in GFAP signal intensity can be seen in the neuron + 10% astrocyte condition, suggesting a decrease in GFAP+ astrocytes following 10 $\mu$M sTHC exposure.

Knowing how molecular makers of neuron and astrocyte populations were affected following 10 $\mu$M sTHC, we wanted to investigate how the OXPHOS machinery changed in response to 10 $\mu$M sTHC. While previous work in the lab found that 1 and 5 mg/kg THC significantly increased the abundance of OXPHOS subunits within total proteins extracted from postnatal hippocampus, we found no significant changes in the OXPHOS subunits cytochrome b-c1 complex subunit 2 [UQCRC2; CIII] and cytochrome c oxidase subunit 1 [MTCO1; CIV] in the sTHC exposed neurons compared to the control (Figure 5A). However, when normalized to TUJ1, the neuron + 10% astrocyte condition saw a significant decrease in UQCRC2 and MTCO1 compared to the neuron + 10% astrocyte DMSO control and a trending and significant decrease in MTCO1 and UQCRC2 when normalized to GFAP. Thus, there is reason to believe that 10 $\mu$M sTHC exposure induces molecular maladaptation of cellular bioenergetics.

# 6. DISCUSSION

The primary objective for this study was to better understand the role astrocytes play following early postnatal hippocampal THC exposure. Beginning with a potential THC mechanism of action, we show that in early postnatal development (P3-P8), we are minimally able to localize $CB_1R$ in the developing hippocampus via *in situ* hybridization. However, this data does not preclude the ability for THC to act within hippocampal astrocyte populations. While THC may act on other G-protein coupled receptors, including the $CB_2R$, the highly lipophilic composition of THC also allows for interactions on the cellular and subcellular membranes (Lutz, 2004) (Mavromoustakos et al., 2019) (Jimenez-Blasco et al., 2020). Further investigation is needed to establish the mechanism of action of THC on early postnatal hippocampal astrocytes.

Though we were unable to confirm an extensive presence of the $CB_1R$ via *in situ* hybridization in early postnatal astrocytes, preliminary data from our group indicated that there were increased s100β and GFAP positive astrocytes in the stratum radiatum of the postnatal hippocampus following THC exposure. This, coupled with the increase in EAAT2 seen in the iTRAQ proteomics data, led us to hypothesize that astrocytes respond to THC by proliferating, differentiating, or migrating into the stratum radiatum of the hippocampus. We chose to test this theory *in vitro* as opposed to *in vivo* as it gave us the ability to better control the environment and testing conditions. Using an EdU staining of early postnatal astrocytes exposed to 1 $\mu$M THC, we show that there are no proliferative effects induced by THC. Immunohistochemical staining with s100β and GFAP also indicated no changes in astrocyte activation or maturity when compared to the control populations *in vitro*.

Being as we found no significant changes in proliferation or differentiation among *in vitro* astrocyte populations, we proposed that hippocampal astroglia may migrate to sensitive areas of the hippocampus to protect neuronal cohorts from THC-induced pathological damage. This hypothesis accounts for the increased astrocyte markers seen in the hippocampus but would also substantiate our gross observation that noted less neuronal death, and therefore cellular debris, when astrocytes were cultured with neurons compared to neurons cultured alone. An unquantified observation of decreased neuronal death 24 hours after neuron and astrocyte were co-cultured in a T-75 flask formed the basis for our *in vitro* neuron and astrocyte co-culture paradigm. Here, we predicted astrocytes will mitigate the decrease in neurite outgrowth and neuronal death that was noted in neuron only cultures, preserving hippocampal neuron populations (Beiersdorf et al., 2020). Indeed, it was shown that with pTHC, the physical presence of 33% astrocytes *in vitro*, as compared to *in vivo* physiological numbers of upward of 50%, significantly protected primary hippocampal neurons from THC-induced cell death (Witcher et al., 2010). This effect was preserved in a similar paradigm with sTHC that isolated the effects of THC and limited the astrocyte quantities to 10% and 20%. Through this data, we show that as little as 10% astrocytes are sufficient to protect neurite outgrowth and neuronal viability, even when exposed to 7.5 $\mu$M and 10 $\mu$M sTHC. This protection and conservation are even greater in the 20% astrocyte condition.

Our *in vitro* findings indicate that astrocyte presence improves neuronal survival following pTHC and sTHC exposure. This data aligns with the current understanding that astrocytes play a

key role in maintaining cell viability and modulating metabolic function through the release of several growth factors including BDNF, GDNF, and NGF (Cabezas et al., 2016). To isolate whether the observed neuronal survival was a factor of physical astrocyte presence or attributed to factors released by astrocytes, our lab plated out a neuron only culture in glial conditioned medium before THC exposure. This medium was prepared in the same manner indicated for astrocyte medium in the methods and was collected and frozen down after incubating with astrocytes for 24 hours. However, the glial conditioned medium was found to be insufficient in reducing neuronal death following exposure to 5 $\mu$M sTHC, suggesting that the neuroprotective effects of astrocytes *in vitro* is not attributed to the release of chemical factors by astrocytes. Instead, our lab finds that the physical presence of astrocytes is key to neuronal survival.

Astrocytes have been shown to respond to brain injury and diseased pathology through reactive gliosis and phagocytic response at the cellular level (Wakida et al., 2018). One study demonstrated that astrocytes engulf cellular debris and apoptotic cells *in vitro,* thereby protecting surrounding neurons from toxic chemicals released upon cell death (Lööv et al., 2012). These findings substantiate the observation that astrocyte presence reduces cellular debris *in vitro*, as seen when comparing Figure 3A to 3D. Additionally, astrocytes play an important role in cellular metabolism. In fact, astrocyte and neuron metabolism is thought to be highly interconnected as the astrocyte-neuron lactate shuttle hypothesis states that lactate produced by glucose metabolism in astrocytes is shuttled into neurons and used as fuel for oxidative phosphorylation in neurons (Rose et al., 2020). Working from previous data collected in the lab that showed alterations in mitochondrial proteins and mitochondrial membrane potential (MMP) in THC-exposed neurons, we asked whether sTHC exposure in the presence and absence of astrocytes would alter OXPHOS machinery. Western blot analysis of neuron and neuron-astrocyte co-cultures found that OXPHOS subunits UQCRC2 and MTCO1 decrease in neuron-astrocyte co-cultures, indicating that there is a downregulation of these select mitochondrial proteins following 10 $\mu$M sTHC exposure. Surprisingly, downregulation of the OXPHOS subunits was not seen in neuron only cultures. We believe this to be attributed to the strong binding of cellular debris to the poly-D-lysine, rendering the OXPHOS proteins unable to be washed away even after neuronal death. This differs from the neuron-astrocyte co-culture as the astrocytes in culture sequester and phagocytose cellular debris and proteins in response to neuronal death (Lööv et al., 2012). In this way, only the OXPHOS subunits in healthy cell populations are detected via western blot whereas OXPHOS subunits and cellular debris are not washed away from the neuron only culture and are detectable via western blot. Overall, findings from the western blot analysis point toward impaired metabolic functioning of astrocytes and neurons, despite the protective function of astrocytes over surrounding neurons.

While we were able to identify that astrocytes provide a neuroprotective effect *in vitro*, future work is needed to understand why greater amounts of astrocytes are seen in specific layers of the hippocampus *in vivo*. We propose that in accordance with the described functions of neuroprotection and removal of cellular debris, astrocytes may migrate and/or activate in areas sensitive to THC within the hippocampus (Lööv et al., 2012). Furthermore, the mechanism by which astrocytes are protecting astrocytes remains poorly understood. There are a couple theories of interest. One hypothesis is that THC accumulates in astrocyte membranes due to its lipophilic character, thereby reducing the THC exposure for nearby neuronal populations (Gill et al., 1976). Another study investigated chemotherapy-induced toxicity and found that astrocytes

improve neuronal survival after cisplatin treatment, improving mitochondrial membrane potential via transfer of mitochondria from astrocytes to neurons (English et al., 2020). Following the methodology established by English et al., it could be possible to label astrocyte mitochondria with a mitochondrial localization sequence and subsequently visualize mitochondrial locations post-THC treatment. Lastly, further work is needed to elucidate the mechanism of action of THC on early postnatal hippocampal astrocytes. Work done by the Marsicano group has identified the presence of astroglial type-1 cannabinoid receptors associated with mitochondrial membranes ($mtCB_1$). When stimulated, $mtCB_1$ was found to impair astrocyte glucose metabolism and impact neuronal function (Jimenez-Blasco et al., 2020). Seeing as we identified changes to select OXPHOS subunits in the neuron-astrocyte co-culture following THC exposure, it follows that activation of astroglial $mtCB_1$ may be responsible for the observed alterations in cellular bioenergetic seen within neuron-astrocyte co-cultures.

In summary, we combine *in situ* hybridization, immunohistochemistry, high resolution microscopy, live cell imaging, and western blotting to demonstrate the relationship between THC, astrocytes, and primary hippocampal neurons. These techniques identified the minimal presence of $CB_1R$ via *in situ* hybridization in early postnatal astrocytes, astrocyte protection of primary neurons following exposure to micromolar concentrations of THC, and THC-induced alterations to cellular metabolism. These findings are important as one study showed that exposure to the smoke of a single hit of 200 mg of cannabis resulted in micromolar concentrations of bioavailable THC in the brain (Poklis et al., 2010). These concentrations only increase over time as subsequent use of THC adds on to the remaining bioavailable THC given its lipophilic storage in the brain for up to 27 days post-THC exposure (Huestis, 2007). As the consumer market pushes increased THC concentrations in plant-derived and synthetic THC preparations, the use of THC for breast feeding mothers and early pediatric care should be used with caution as data from our study suggests alterations to early postnatal hippocampal cell populations *in vitro*. Overall, this study establishes a preliminary platform for future work to further derive the relationship between astrocytes and neurons, specifically how astrocytes protect primary neurons from THC-induced damage.

# 7. REFERENCES


Adams R. (1942). Marihuana: Harvey Lecture, February 19, 1942. *Bulletin of the New York Academy of Medicine*, *18*(11), 705–730.

Allen, John R, et al. "Single Molecule Localization Microscopy for Superresolution." *Journal of Optics,* vol. 15, no. 9, 2013, p. 094001., https://doi.org/10.1088/2040-8978/15/9/094001.

Anlauf, E., & Derouiche, A. (2013). Glutamine synthetase as an astrocytic marker: its cell type and vesicle localization. *Frontiers in endocrinology*, *4*, 144. https://doi.org/10.3389/fendo.2013.00144

Astley, S. J., & Little, R. E. (1990). Maternal marijuana use during lactation and infant development at one year. *Neurotoxicology and teratology*, *12*(2), 161–168. https://doi.org/10.1016/0892-0362(90)90129-z

Becker, M. P., Collins, P. F., Schultz, A., Urošević, S., Schmaling, B., & Luciana, M. (2018). Longitudinal changes in cognition in young adult cannabis users. *Journal of clinical and experimental neuropsychology*, *40*(6), 529–543. https://doi.org/10.1080/13803395.2017.1385729

Beiersdorf, J., Hevesi, Z., Calvigioni, D., Pyszkowski, J., Romanov, R., Szodorai, E., Lubec, G., Shirran, S., Botting, C. H., Kasper, S., Guy, G. W., Gray, R., Di Marzo, V., Harkany, T., & Keimpema, E. (2020). Adverse effects of Δ9-tetrahydrocannabinol on neuronal bioenergetics during postnatal development. *JCI insight*, *5*(23), e135418. https://doi.org/10.1172/jci.insight.135418

Bénard, G., Massa, F., Puente, N., Lourenço, J., Bellocchio, L., Soria-Gómez, E., Matias, I., Delamarre, A., Metna-Laurent, M., Cannich, A., Hebert-Chatelain, E., Mulle, C., Ortega-Gutiérrez, S., Martín-Fontecha, M., Klugmann, M., Guggenhuber, S., Lutz, B., Gertsch, J., Chaouloff, F., López-Rodríguez, M. L., … Marsicano, G. (2012). Mitochondrial $CB_1$ receptors regulate neuronal energy metabolism. *Nature neuroscience*, *15*(4), 558–564. https://doi.org/10.1038/nn.3053

Bliss, T. V., & Collingridge, G. L. (1993). A synaptic model of memory: long-term potentiation in the hippocampus. *Nature*, *361*(6407), 31–39. https://doi.org/10.1038/361031a0

Cabezas, R., Avila-Rodriguez, M., Vega-Vela, N. E., Echeverria, V., González, J., Hidalgo, O. A., Santos, A. B., Aliev, G., & Barreto, G. E. (2016). Growth Factors and Astrocytes Metabolism: Possible Roles for Platelet Derived Growth Factor. *Medicinal chemistry (Shariqah (United Arab Emirates))*, *12*(3), 204–210. https://doi.org/10.2174/1573406411666151019120444

Castellanos-Ryan, N., Pingault, J. B., Parent, S., Vitaro, F., Tremblay, R. E., & Séguin, J. R. (2017). Adolescent cannabis use, change in neurocognitive function, and high-school graduation: A longitudinal study from early adolescence to young adulthood. *Development and psychopathology*, *29*(4), 1253–1266. https://doi.org/10.1017/S0954579416001280

Chayasirisobhon S. (2020). Mechanisms of Action and Pharmacokinetics of Cannabis. *The Permanente journal*, *25*, 1–3. https://doi.org/10.7812/TPP/19.200

Chen, R., Zhang, J., Fan, N., Teng, Z. Q., Wu, Y., Yang, H., Tang, Y. P., Sun, H., Song, Y., & Chen, C. (2013). Δ9-THC-caused synaptic and memory impairments are mediated through COX-2 signaling. *Cell*, *155*(5), 1154–1165. https://doi.org/10.1016/j.cell.2013.10.042

Compton, W. M., Han, B., Jones, C. M., Blanco, C., & Hughes, A. (2016). Marijuana use and use disorders in adults in the USA, 2002-14: analysis of annual cross-sectional surveys. *The lancet. Psychiatry*, *3*(10), 954–964. https://doi.org/10.1016/S2215-0366(16)30208-5

Crocq M. A. (2020). History of cannabis and the endocannabinoid system. *Dialogues in clinical neuroscience*, *22*(3), 223–228. https://doi.org/10.31887/DCNS.2020.22.3/mcrocq

Crittenden, J. R., Yoshida, T., Venu, S., Mahar, A., & Graybiel, A. M. (2022). Cannabinoid Receptor 1 Is Required for Neurodevelopment of Striosome-Dendron Bouquets. *eNeuro*, *9*(2), ENEURO.0318-21.2022. https://doi.org/10.1523/ENEURO.0318-21.2022

Devane, W. A., Dysarz, F. A., 3rd, Johnson, M. R., Melvin, L. S., & Howlett, A. C. (1988). Determination and characterization of a cannabinoid receptor in rat brain. *Molecular pharmacology*, *34*(5), 605–613.

Devane, W. A., Hanus, L., Breuer, A., Pertwee, R. G., Stevenson, L. A., Griffin, G., Gibson, D., Mandelbaum, A., Etinger, A., & Mechoulam, R. (1992). Isolation and structure of a brain constituent that binds to the cannabinoid receptor. *Science (New York, N.Y.)*, *258*(5090), 1946–1949. https://doi.org/10.1126/science.1470919

English, K., Shepherd, A., Uzor, N. E., Trinh, R., Kavelaars, A., & Heijnen, C. J. (2020). Astrocytes rescue neuronal health after cisplatin treatment through mitochondrial transfer. *Acta neuropathologica communications*, *8*(1), 36. https://doi.org/10.1186/s40478-020-00897-7

Escartin, C., Galea, E., Lakatos, A., O'Callaghan, J. P., Petzold, G. C., Serrano-Pozo, A., Steinhäuser, C., Volterra, A., Carmignoto, G., Agarwal, A., Allen, N. J., Araque, A., Barbeito, L., Barzilai, A., Bergles, D. E., Bonvento, G., Butt, A. M., Chen, W. T., Cohen-Salmon, M., Cunningham, C., … Verkhratsky, A. (2021). Reactive astrocyte nomenclature, definitions, and future directions. *Nature neuroscience*, *24*(3), 312–325. https://doi.org/10.1038/s41593-020-00783-4

Felder, C. C., & Glass, M. (1998). Cannabinoid receptors and their endogenous agonists. *Annual review of pharmacology and toxicology*, *38*, 179–200. https://doi.org/10.1146/annurev.pharmtox.38.1.179

Fišar, Z., Singh, N., & Hroudová, J. (2014). Cannabinoid-induced changes in respiration of brain mitochondria. *Toxicology letters*, *231*(1), 62–71. https://doi.org/10.1016/j.toxlet.2014.09.002

Fuerte-Hortigón, A., Gonçalves, J., Zeballos, L., Masa, R., Gómez-Nieto, R., & López, D. E. (2021). Distribution of the Cannabinoid Receptor Type 1 in the Brain of the Genetically Audiogenic Seizure-Prone Hamster GASH/Sal. *Frontiers in behavioral neuroscience*, *15*, 613798. https://doi.org/10.3389/fnbeh.2021.613798

Gill EW, Lawrence DK. The physicochemical mode of action of THC on cell membranes. In: Braude MC, Szara S eds. *The Pharmacology of Marihuana*. 1976:147–155.

Gómez Del Pulgar, T., De Ceballos, M. L., Guzmán, M., & Velasco, G. (2002). Cannabinoids protect astrocytes from ceramide-induced apoptosis through the phosphatidylinositol 3-kinase/protein kinase B pathway. *The Journal of biological chemistry*, *277*(39), 36527–36533. https://doi.org/10.1074/jbc.M205797200

Hall, W., & Lynskey, M. (2020). Assessing the public health impacts of legalizing recreational cannabis use: the US experience. *World psychiatry: official journal of the World Psychiatric Association (WPA)*, *19*(2), 179–186. https://doi.org/10.1002/wps.20735

Hillard, C. J., Harris, R. A., & Bloom, A. S. (1985). Effects of the cannabinoids on physical properties of brain membranes and phospholipid vesicles: fluorescence studies. *The Journal of pharmacology and experimental therapeutics*, *232*(3), 579–588.

Hol, E. M., & Pekny, M. (2015). Glial fibrillary acidic protein (GFAP) and the astrocyte intermediate filament system in diseases of the central nervous system. *Current opinion in cell biology*, *32*, 121–130. https://doi.org/10.1016/j.ceb.2015.02.004

Howlett, A. C., Barth, F., Bonner, T. I., Cabral, G., Casellas, P., Devane, W. A., Felder, C. C., Herkenham, M., Mackie, K., Martin, B. R., Mechoulam, R., & Pertwee, R. G. (2002). International Union of Pharmacology. XXVII. Classification of cannabinoid receptors. *Pharmacological reviews*, *54*(2), 161–202. https://doi.org/10.1124/pr.54.2.161

Huestis M. A. (2007). Human cannabinoid pharmacokinetics. *Chemistry & biodiversity*, *4*(8), 1770–1804. https://doi.org/10.1002/cbdv.200790152

Keimpema, E., Mackie, K., & Harkany, T. (2011). Molecular model of cannabis sensitivity in developing neuronal circuits. *Trends in pharmacological sciences*, *32*(9), 551–561. https://doi.org/10.1016/j.tips.2011.05.004

Lee, E., & Chung, W. S. (2019). Glial Control of Synapse Number in Healthy and Diseased Brain. *Frontiers in cellular neuroscience*, *13*, 42. https://doi.org/10.3389/fncel.2019.00042

Lee, S., Choi, K., Ahn, H., Song, K., Choe, J., & Lee, I. (2005). TuJ1 (class III beta-tubulin) expression suggests dynamic redistribution of follicular dendritic cells in lymphoid tissue. *European journal of cell biology*, *84*(2-3), 453–459. https://doi.org/10.1016/j.ejcb.2004.11.001

Leishman, E., Murphy, M., Mackie, K., & Bradshaw, H. B. (2018). $\Delta^9$-Tetrahydrocannabinol changes the brain lipidome and transcriptome differentially in the adolescent and the adult. *Biochimica et biophysica acta. Molecular and cell biology of lipids*, *1863*(5), 479–492. https://doi.org/10.1016/j.bbalip.2018.02.001

Lööv, C., Hillered, L., Ebendal, T., & Erlandsson, A. (2012). Engulfing astrocytes protect neurons from contact-induced apoptosis following injury. *PloS one*, *7*(3), e33090. https://doi.org/10.1371/journal.pone.0033090

Lu, H. C., & Mackie, K. (2016). An Introduction to the Endogenous Cannabinoid System. *Biological psychiatry*, *79*(7), 516–525. https://doi.org/10.1016/j.biopsych.2015.07.028

Lutz B. (2004). On-demand activation of the endocannabinoid system in the control of neuronal excitability and epileptiform seizures. *Biochemical pharmacology*, *68*(9), 1691–1698. https://doi.org/10.1016/j.bcp.2004.07.007

Lynskey, M. T., Agrawal, A., Henders, A., Nelson, E. C., Madden, P. A., & Martin, N. G. (2012). An Australian twin study of cannabis and other illicit drug use and misuse, and other psychopathology. *Twin research and human genetics: the official journal of the International Society for Twin Studies*, *15*(5), 631–641. https://doi.org/10.1017/thg.2012.41

Maglóczky, Z., Tóth, K., Karlócai, R., Nagy, S., Eross, L., Czirják, S., Vajda, J., Rásonyi, G., Kelemen, A., Juhos, V., Halász, P., Mackie, K., & Freund, T. F. (2010). Dynamic changes of CB1-receptor expression in hippocampi of epileptic mice and humans. *Epilepsia*, *51 Suppl 3*(Suppl 3), 115–120. https://doi.org/10.1111/j.1528-1167.2010.02624.x

Mavromoustakos, T., & Daliani, I. (1999). Effects of cannabinoids in membrane bilayers containing cholesterol. *Biochimica et biophysica acta*, *1420*(1-2), 252–265. https://doi.org/10.1016/s0005-2736(99)00106-6

Mechoulam, R., & Gaoni, Y. (1965). A total synthesis of DL-Delta-1-tetrahydrocannabinol, the active constituent of hashish. *Journal of the American Chemical Society*, *87*, 3273–3275. https://doi.org/10.1021/ja01092a065

Melser, S., Pagano Zottola, A. C., Serrat, R., Puente, N., Grandes, P., Marsicano, G., & Hebert-Chatelain, E. (2017). Functional Analysis of Mitochondrial CB1 Cannabinoid Receptors (mtCB1) in the Brain. *Methods in enzymology*, *593*, 143–174. https://doi.org/10.1016/bs.mie.2017.06.023

Morozov, Y. M., Torii, M., & Rakic, P. (2009). Origin, early commitment, migratory routes, and destination of cannabinoid type 1 receptor-containing interneurons. *Cerebral cortex (New York, N.Y.: 1991)*, *19 Suppl 1*(Suppl 1), i78–i89. https://doi.org/10.1093/cercor/bhp028

Moulson, A. J., Squair, J. W., Franklin, R., Tetzlaff, W., & Assinck, P. (2021). Diversity of Reactive Astrogliosis in CNS Pathology: Heterogeneity or Plasticity?. *Frontiers in cellular neuroscience*, *15*, 703810. https://doi.org/10.3389/fncel.2021.703810.

Mulder, J., Aguado, T., Keimpema, E., Barabás, K., Ballester Rosado, C. J., Nguyen, L., Monory, K., Marsicano, G., Di Marzo, V., Hurd, Y. L., Guillemot, F., Mackie, K., Lutz, B., Guzmán, M., Lu, H. C., Galve-Roperh, I., & Harkany, T. (2008). Endocannabinoid signaling controls pyramidal cell specification and long-range axon patterning. *Proceedings of the National Academy of Sciences of the United States of America*, *105*(25), 8760–8765. https://doi.org/10.1073/pnas.0803545105

Navarrete, F., García-Gutiérrez, M. S., Gasparyan, A., Austrich-Olivares, A., Femenía, T., & Manzanares, J. (2020). Cannabis Use in Pregnant and Breastfeeding Women: Behavioral and Neurobiological Consequences. *Frontiers in psychiatry*, *11*, 586447. https://doi.org/10.3389/fpsyt.2020.586447

Navarrete, M., Díez, A., & Araque, A. (2014). Astrocytes in endocannabinoid signalling. *Philosophical transactions of the Royal Society of London. Series B, Biological sciences*, *369*(1654), 20130599. https://doi.org/10.1098/rstb.2013.0599

Orr, C., Spechler, P., Cao, Z., Albaugh, M., Chaarani, B., Mackey, S., D'Souza, D., Allgaier, N., Banaschewski, T., Bokde, A., Bromberg, U., Büchel, C., Burke Quinlan, E., Conrod, P., Desrivières, S., Flor, H., Frouin, V., Gowland, P., Heinz, A., Ittermann, B., … Garavan, H. (2019). Grey Matter Volume Differences Associated with Extremely Low Levels of Cannabis Use in Adolescence. *The Journal of neuroscience: the official journal of the Society for Neuroscience*, *39*(10), 1817–1827. https://doi.org/10.1523/JNEUROSCI.3375-17.2018

O'Shaughnessy W. B. (1843). On the Preparations of the Indian Hemp, or Gunjah: Cannabis Indica Their Effects on the Animal System in Health, and their Utility in the Treatment of Tetanus and other Convulsive Diseases. *Provincial Medical Journal and Retrospect of the Medical Sciences*, *5*(123), 363–369.

Pertwee R. ed. *Handbook of Cannabis. Oxford University Press; 2014. Available at: http://www.oxfordscholarship.eom/view/10.1093/acprof:oso/9780199662685.001.0001/acprof-9780199662685. Published online January 2015.*

Pertwee R. G. (2008). The diverse CB1 and CB2 receptor pharmacology of three plant cannabinoids: delta9-tetrahydrocannabinol, cannabidiol and delta9-tetrahydrocannabivarin. *British journal of pharmacology*, *153*(2), 199–215. https://doi.org/10.1038/sj.bjp.0707442

Poklis, J. L., Thompson, C. C., Long, K. A., Lichtman, A. H., & Poklis, A. (2010). Disposition of cannabichromene, cannabidiol, and $\Delta^9$-tetrahydrocannabinol and its metabolites in mouse brain following marijuana inhalation determined by high-performance liquid chromatography-tandem mass spectrometry. *Journal of analytical toxicology*, *34*(8), 516–520. https://doi.org/10.1093/jat/34.8.516

Raponi, E., Agenes, F., Delphin, C., Assard, N., Baudier, J., Legraverend, C., & Deloulme, J. C. (2007). S100B expression defines a state in which GFAP-expressing cells lose their neural stem

cell potential and acquire a more mature developmental stage. *Glia*, *55*(2), 165–177. https://doi.org/10.1002/glia.20445

Rodriguez, J. J., Mackie, K., & Pickel, V. M. (2001). Ultrastructural localization of the CB1 cannabinoid receptor in mu-opioid receptor patches of the rat Caudate putamen nucleus. *The Journal of neuroscience: the official journal of the Society for Neuroscience*, *21*(3), 823–833. https://doi.org/10.1523/JNEUROSCI.21-03-00823.2001

Rose, J., Brian, C., Pappa, A., Panayiotidis, M. I., & Franco, R. (2020). Mitochondrial Metabolism in Astrocytes Regulates Brain Bioenergetics, Neurotransmission and Redox Balance. *Frontiers in neuroscience*, *14*, 536682. https://doi.org/10.3389/fnins.2020.536682

Russo E. B. (2011). Taming THC: potential cannabis synergy and phytocannabinoid-terpenoid entourage effects. *British journal of pharmacology*, *163*(7), 1344–1364. https://doi.org/10.1111/j.1476-5381.2011.01238.x

Salio, C., Doly, S., Fischer, J., Franzoni, M. F., & Conrath, M. (2002). Neuronal and astrocytic localization of the cannabinoid receptor-1 in the dorsal horn of the rat spinal cord. *Neuroscience letters*, *329*(1), 13–16. https://doi.org/10.1016/s0304-3940(02)00549-9

Sarafian, T. A., Kouyoumjian, S., Khoshaghideh, F., Tashkin, D. P., & Roth, M. D. (2003). Delta 9-tetrahydrocannabinol disrupts mitochondrial function and cell energetics. *American journal of physiology. Lung cellular and molecular physiology*, *284*(2), L298–L306. https://doi.org/10.1152/ajplung.00157.2002

Scott, J. C., Wolf, D. H., Calkins, M. E., Bach, E. C., Weidner, J., Ruparel, K., Moore, T. M., Jones, J. D., Jackson, C. T., Gur, R. E., & Gur, R. C. (2017). Cognitive functioning of adolescent and young adult cannabis users in the Philadelphia Neurodevelopmental Cohort. *Psychology of addictive behaviors: journal of the Society of Psychologists in Addictive Behaviors*, *31*(4), 423–434. https://doi.org/10.1037/adb0000268

Sims, N. R., & Yew, W. P. (2017). Reactive astrogliosis in stroke: Contributions of astrocytes to recovery of neurological function. *Neurochemistry international*, *107*, 88–103. https://doi.org/10.1016/j.neuint.2016.12.016

Stella N. (2004). Cannabinoid signaling in glial cells. *Glia*, *48*(4), 267–277. https://doi.org/10.1002/glia.20084

Sun, X., & Dey, S. K. (2008). Aspects of endocannabinoid signaling in periimplantation biology. *Molecular and cellular endocrinology*, *286*(1-2 Suppl 1), S3–S11. https://doi.org/10.1016/j.mce.2008.01.002

Timper, K., Del Río-Martín, A., Cremer, A. L., Bremser, S., Alber, J., Giavalisco, P., Varela, L., Heilinger, C., Nolte, H., Trifunovic, A., Horvath, T. L., Kloppenburg, P., Backes, H., & Brüning, J. C. (2020). GLP-1 Receptor Signaling in Astrocytes Regulates Fatty Acid Oxidation,

Mitochondrial Integrity, and Function. *Cell metabolism*, *31*(6), 1189–1205.e13. https://doi.org/10.1016/j.cmet.2020.05.001

U.S. Department of Health and Human Services. (2022, June 3). *Cannabis (marijuana) potency*. National Institutes of Health. Retrieved September 8, 2022, from https://nida.nih.gov/research-topics/marijuana/cannabis-marijuana-potency

Vitalis, T., Lainé, J., Simon, A., Roland, A., Leterrier, C., & Lenkei, Z. (2008). The type 1 cannabinoid receptor is highly expressed in embryonic cortical projection neurons and negatively regulates neurite growth in vitro. *The European journal of neuroscience*, *28*(9), 1705–1718. https://doi.org/10.1111/j.1460-9568.2008.06484.x

von Bartheld, C. S., Bahney, J., & Herculano-Houzel, S. (2016). The search for true numbers of neurons and glial cells in the human brain: A review of 150 years of cell counting. *The Journal of comparative neurology*, *524*(18), 3865–3895. https://doi.org/10.1002/cne.24040

Wakida, N. M., Cruz, G., Ro, C. C., Moncada, E. G., Khatibzadeh, N., Flanagan, L. A., & Berns, M. W. (2018). Phagocytic response of astrocytes to damaged neighboring cells. *PloS one*, *13*(4), e0196153. https://doi.org/10.1371/journal.pone.0196153

Weber, B., & Barros, L. F. (2015). The Astrocyte: Powerhouse and Recycling Center. *Cold Spring Harbor perspectives in biology*, *7*(12), a020396. https://doi.org/10.1101/cshperspect.a020396

Witcher, M. R., Park, Y. D., Lee, M. R., Sharma, S., Harris, K. M., & Kirov, S. A. (2010). Three-dimensional relationships between perisynaptic astroglia and human hippocampal synapses. *Glia*, *58*(5), 572–587. https://doi.org/10.1002/glia.20946

Yang, H., An, J., Choi, I., Lee, K., Park, S. M., Jou, I., & Joe, E. H. (2020). Region-specific astrogliosis: differential vessel formation contributes to different patterns of astrogliosis in the cortex and striatum. *Molecular brain*, *13*(1), 103. https://doi.org/10.1186/s13041-020-00642-0

Zhang, S., Wu, M., Peng, C., Zhao, G., & Gu, R. (2017). GFAP expression in injured astrocytes in rats. *Experimental and therapeutic medicine*, *14*(3), 1905–1908. https://doi.org/10.3892/etm.2017.4760

Zhang, Z., Zheng, X., Zeng, D. D., & Leischow, S. J. (2016). Tracking Dabbing Using Search Query Surveillance: A Case Study in the United States. *Journal of medical Internet research*, *18*(9), e252. https://doi.org/10.2196/jmir.5802